



Autonomous seawater $p\text{CO}_2$ and pH time series from 40 surface buoys and the emergence of anthropogenic trends

Adrienne J. Sutton¹, Richard A. Feely¹, Stacy Maenner-Jones¹, Sylvia Musielwicz^{1,2}, John Osborne^{1,2}, Colin Dietrich^{1,2}, Natalie Monacci³, Jessica Cross¹, Randy Bott¹, Alex Kozyr⁴

5 ¹Pacific Marine Environmental Laboratory, National Oceanic and Atmospheric Administration, Seattle, Washington, USA

²Joint Institute for the Study of the Atmosphere and Ocean, University of Washington, Seattle, Washington, USA

³Ocean Acidification Research Center, University of Alaska Fairbanks, Fairbanks, Alaska, USA

⁴National Centers for Environmental Information, National Oceanic and Atmospheric Administration, Silver Spring, Maryland, USA

10 *Correspondence to:* Adrienne J. Sutton (adrienne.sutton@noaa.gov)

Abstract. Ship-based time series, some now approaching over three decades long, are critical climate records that have dramatically improved our ability to characterize natural and anthropogenic drivers of ocean CO_2 uptake and biogeochemical processes. Advancements in autonomous ocean carbon observing technology over the last two decades have led to the expansion of fixed time series stations with the added capability of characterizing sub-seasonal variability. Here we present a data product of 40 autonomous moored surface ocean $p\text{CO}_2$ (partial pressure of CO_2) and pH time series established between 2004 and 2013. These time series characterize a wide range of seawater $p\text{CO}_2$ and pH conditions in different oceanic (17 sites) and coastal (12 sites) regimes including coral reefs (11 sites). With well-constrained daily to interannual variability and an estimate of decadal variability, these data suggest the length of time series necessary to detect an anthropogenic trend in seawater $p\text{CO}_2$ and pH varies from 8 to 15 years at the open ocean sites, 16 to 41 years at the coastal sites, and 9 to 22 years at the coral reef sites. Only two open ocean $p\text{CO}_2$ time series, WHOTS in the subtropical North Pacific and Stratus in the South Pacific gyre, are longer than the estimated time of emergence, and deseasoned monthly means show anthropogenic trends of $1.9 \pm 0.3 \mu\text{atm yr}^{-1}$ and $1.6 \pm 0.3 \mu\text{atm yr}^{-1}$, respectively. In the future, it is possible that updates to this product will allow for estimating anthropogenic trends at more sites; however, the product currently provides a valuable tool in an accessible format for evaluating climatology and natural variability of surface ocean carbonate chemistry in a variety of regions. Data are available at <https://doi.org/10.7289/V5DB8043> and <https://www.nodc.noaa.gov/ocads/oceans/Moorings/ndp097.html>.

1 Introduction

Biogeochemical cycling leads to remarkable temporal and spatial variability of carbon in the mixed layer of the global ocean and throughout coastal seas. The ocean carbon cycle is heavily influenced by local physical conditions and biological processes, basin-wide circulation patterns, and fluxes between the ocean and land/atmosphere. Since the industrial period, increasing atmospheric carbon dioxide (CO_2) has been an additional forcing on ocean biogeochemistry, with the ocean absorbing roughly 30% of anthropogenic CO_2 (Khatalwala et al., 2013; Le Quéré et al., 2018). The resulting decrease of seawater pH and carbonate ion concentration, referred to as ocean acidification, has the potential to impact marine life such as calcifying organisms (Bednaršek et al., 2017b; Davis et al., 2017; Eyre et al., 2018; Gattuso et al., 2015). Shellfish, shallow-water tropical corals, and calcareous plankton are a few examples of economically and ecologically important marine calcifiers.

Open ocean observations have shown that the inorganic carbon chemistry of the surface ocean is changing globally at a mean rate consistent with atmospheric CO_2 increases of approximately $2.0 \mu\text{atm yr}^{-1}$ (Bates et al., 2014; Takahashi et al., 2009; Wanninkhof et al., 2013). However, natural and anthropogenic processes can magnify temporal and spatial variability in some regions,



especially coastal systems through eutrophication, freshwater input, exchange with tidal wetlands and the sea floor, seasonal biological productivity, and coastal upwelling (Bauer et al., 2013). This magnification of natural variability can obscure detection and attribution of long-term change in coastal ocean carbon.

5 Efforts to observe and predict ocean acidification impact to marine ecosystems must be paired with an understanding of both the natural and anthropogenic processes that control the ocean carbonate system. Marine life experience highly heterogeneous seawater carbon chemistry conditions, and it is unclear what exact conditions in the natural environment will lead to physiological responses (Hofmann et al., 2010), although responses associated with carbonate conditions have been observed (Barton et al., 2012, 2015; Bednaršek et al., 2017a, 2016, 2014; Reum et al., 2015). Observations show that present-day surface seawater pH and aragonite saturation state conditions throughout most of the open ocean exceed the natural range of preindustrial variability, and in some coastal ecosystems, known biological thresholds for shellfish larvae are exceeded during certain times of the seasonal cycle (Sutton et al., 2016). Are these present-day conditions impacting marine life in the natural environment? How will intensity, frequency, and duration of seasonal corrosive events change as surface seawater pH and aragonite saturation state continue to decline and influence other processes of the biogeochemical cycle in the coastal zone? Paired chemical and biological observations at timescales relevant to biological processes, such as food availability, seasonal spawning, larval growth, and recruitment, can be one tool for identifying and tracking the response of marine life to ocean acidification.

10 Long-term, sustained time series observations resolving diurnal to seasonal conditions encompass many timescales relevant to these biological processes and can characterize both natural variability and anthropogenic change in ocean carbon. These observations fill a unique niche in ocean observing as they can serve as sites of multidisciplinary observations and process studies, high-quality reference stations for validating and assessing satellite measurements and earth system models, and test beds for developing and evaluating new ocean sensing technology. If of sufficient length and measurement quality to detect the anthropogenic signal above the noise (i.e., the natural variability of the carbon system), these observations can also serve as critical climate records.

20 Here we introduce time series data from 40 moored stations in open ocean, coastal, and coral reef environments. These time series include 3-hourly autonomous measurements of surface seawater temperature (SST), salinity (SSS), partial pressure of atmospheric and seawater CO_2 ($p\text{CO}_2$), mole fraction of atmospheric CO_2 ($x\text{CO}_2$), and seawater pH. This data product was developed to provide easy access to uninterrupted time series of high-quality $p\text{CO}_2$ and pH data for those who do not require the detailed deployment-level information archived at the National Centers for Environmental Information (NCEI; https://www.nodc.noaa.gov/ocads/oceans/time_series_moorings.html). Here we present an overview of the seasonal variability to long-term trends revealed in the $p\text{CO}_2$ and pH observations as well as an estimate of the length of time series required to detect an anthropogenic signal at each location.

2 Methods

2.1 Site and sensor description

35 The 40 fixed time series stations are located in the Pacific (29), Atlantic (9), Indian (1), and Southern (1) ocean basins in open ocean (17), coastal (12), and coral reef (11) ecosystems (Table 1; Fig. 1). All surface ocean $p\text{CO}_2$ and pH time series were established between 2004 and 2013. Thirty-three of these stations are active, while three have been moved to nearby locations better representing regional biogeochemical processes and four have been discontinued due to lack of sustained funding. The range of support and partnerships for maintaining these moored time series is extensive; see Acknowledgements for details.



A Moored Autonomous $p\text{CO}_2$ (MAPCO₂) system measuring marine boundary layer air at 0.5–1 m height and seawater at <0.5 m depth is deployed at each fixed time series site (Sutton et al., 2014b). The MAPCO₂ systems measure $x\text{CO}_2$ in equilibrium with surface seawater by a nondispersive infrared gas analyzer (LI-820, LI-COR) calibrated prior to each measurement with a reference gas traceable to World Meteorological Organization standards. Seawater $x\text{CO}_2$ equilibration occurs by cycling a closed loop of air through an equilibrator at the sea surface for 10 minutes. Each time series site has either a Sea-Bird Electronics (SBE) 16plus V2 Sea-CAT or a SBE 37 MicroCAT deployed at approximately 0.5 m measuring SST and SSS. These measurements are used to calculate $p\text{CO}_2$ and the fugacity of CO_2 ($f\text{CO}_2$) consistent with standard operating procedures (Dickson et al., 2007; Weiss, 1974). Total estimated uncertainties of the resulting $p\text{CO}_2$ measurements are <2 μatm for seawater $p\text{CO}_2$ and <1 μatm for air $p\text{CO}_2$. For a detailed description of the MAPCO₂ methodology, calculations, data reduction, and data quality control, see Sutton et al. (2014b).

In addition to $p\text{CO}_2$, SST, and SSS, 17 of the time series also include seawater pH measurements at 0.5 m depth. These measurements are made by either the spectrophotometric-based Sunburst SAMI pH sensors (Seidel et al., 2008) or ion sensitive field effect transistor-based SeaFET pH sensors (Bresnahan et al., 2014; Martz et al., 2010). Field-based sensor validation suggests these sensors (once calibrated and adjusted in the case of the SeaFET) have a total uncertainty of <0.02 in this surface buoy application (Sutton et al., 2016). At 3-hourly sampling intervals, this configuration of MAPCO₂ and associated sensors are typically deployed for one year before replacement. All seawater pH data are in the total scale.

2.2 Data product description

All post-calibrated and quality-controlled data are archived at NCEI: https://www.nodc.noaa.gov/ocads/oceans/time_series_moorings.html. For each site, an annual deployment has the following files: 1) 3-hourly MAPCO₂ and associated data, including measured parameters such as humidity and atmospheric pressure so data users can recalculate $p\text{CO}_2$ if desired; 2) data quality flag (QF) log that identifies and describes likely bad (QF = 3) or bad (QF = 4) CO_2 and pH data included in the data set; and 3) a metadata file with deployment-level information such as reference gas value and MAPCO₂ air value comparisons to the GLOBALVIEW-CO₂ Marine Boundary Layer (MBL) product (GLOBALVIEW-CO₂, 2013). See Sutton et al. (2014b) for a detailed description of this deployment-level archived information. In addition to archival at NCEI, these deployment-level mooring data sets are also included in the annual Surface Ocean CO₂ Atlas data product (Bakker et al., 2016).

The data product presented here is a compiled and simplified time series developed from these deployment-level archived files. Each fixed moored location has one file with a header including the following basic metadata: 1) data source and contact information; 2) data use request; 3) data product citation; 4) time series name, time range, coordinates; 5) description of variables; 6) methodology references; and 7) links to deployment-level archived data and metadata at NCEI. Following the header, each fixed moored time series file includes the full time series of SST, SSS, seawater $p\text{CO}_2$, air $p\text{CO}_2$, air $x\text{CO}_2$, and pH with associated timestamp.

The time series data product only includes data from the original deployment-level data files assigned QF = 2 (good data). Any missing value or value assigned QF of 3 or 4 in the original deployment-level data are replaced with “NaN” in the time series product. Of the data assigned QF of 2, 3, or 4, the good data (QF = 2) retained in this data product comprise 96% of all seawater $p\text{CO}_2$ values and 88% of all seawater pH values. Missing or bad SST or SSS data further reduce the quantity of seawater $p\text{CO}_2$ values to 85% compared to the archived deployment-level data. Data users interested in all available $x\text{CO}_2$ and pH data should continue to retrieve deployment-level data from the NCEI archive: https://www.nodc.noaa.gov/ocads/oceans/time_series_moorings.html.



Two time series locations are exceptions. Because 3-hourly SST and SSS are not available for the Twanoh and Dabob sites, the data archived at NCEI for those two sites includes $x\text{CO}_2$ (dry) air and seawater values but not calculated $p\text{CO}_2$. In order to calculate $p\text{CO}_2$ for those sites, the data user can incorporate atmospheric pressure, SST, and SSS from other sources. Atmospheric pressure at 3-hourly intervals can be found in the deployment-level archived data files at NCEI. Other data sources, including 2-hourly SST and SSS data at both Twanoh and Dabob, can also be located through the data portal of the Northwest Association of Networked Ocean Observing Systems: <http://nvs.nanoos.org/>. Since interpolating 2-hourly data with the 3-hourly MAPCO₂ data requires making assumptions about temporal variability that may vary according to the research interests of the data user, data from these two locations are only available in the deployment-level data files archived at NCEI.

This data product has been developed to provide easier access to quality-assured seawater $p\text{CO}_2$ and pH data and broaden the user base of these data. This data product is ideal for modelers interested in using fixed time series data to validate earth system model output or other data users accustomed to working with ship-based time series data. It also makes the time series more accessible to students, researchers from other disciplines, and marine resource managers who may not have a carbon chemistry background or the resources necessary to process and interpret the more detailed deployment-level data.

2.3 Statistical analyses

Descriptive statistics from these times series products are presented here to compare variability across the 40 locations. Seasonal amplitude is the difference in the mean of all observations during winter and summer. For Northern Hemisphere sites, winter is defined as December, January, and February, and summer is June, July, and August (vice versa for Southern Hemisphere sites).

The climatological mean is derived by averaging means for each of the twelve months over the composite, multiyear time series. Interannual variability (IAV) is presented as the standard deviation of individual yearly means throughout the time series. In the case of missing observations, climatological monthly means are substituted to calculate yearly means for IAV. This approach seeks to minimize the impact of data gaps on the IAV estimates.

The seasonal cycle is removed from the data using the deseasonization method described in detail in Bates (2001) and Takahashi et al. (2009). This method results in a time series of monthly anomalies, which are monthly residuals after correcting for the climatological monthly means.

Time of emergence (ToE) is a statistical method that, when applied to environmental data, estimates the number of years necessary in a time series to detect an anthropogenic signal over the noise (i.e., natural variability). This method has been used to determine ToE from, for example, chlorophyll satellite records (Henson et al., 2010) and ocean biogeochemical models (Lovenduski et al., 2015). ToE_{ts} (in years) of each time series is derived using the method of Weatherhead et al. (1998):

$$ToE_{ts} = \left(\frac{3.3\sigma N}{|\omega|} \sqrt{\frac{1+\phi}{1-\phi}} \right)^{2/3} \quad (1)$$

where σN and ϕ are the standard deviation and autocorrelation of monthly anomalies, respectively, and ω is the anthropogenic signal of 2 $\mu\text{atm } p\text{CO}_2$ or 0.002 pH per year, assuming surface seawater in equilibrium with the global mean rate of atmospheric CO₂ increase. This method results in a 90% probability (dictated by the factor of 3.3 in Eq. 1) of trend detection by the estimated ToE_{ts} at the 95% confidence interval. Uncertainty in ToE_{ts}, u_{ToE} , is calculated by:

$$u_{ToE} = ToE_{ts} \times e^B \quad (2)$$



where B is the uncertainty factor calculated using the method of Weatherhead et al. (1998). Uncertainty is based on the number of months (m) in the time series and autocorrelation of monthly anomalies (ϕ):

$$B = \frac{4}{3\sqrt{m}} \sqrt{\frac{1+\phi}{1-\phi}} \quad (3)$$

While most of the moored time series characterize diurnal to interannual variability of surface ocean $p\text{CO}_2$ at each location, low frequency decadal variability is not yet fully captured in these ≤ 12 year time series and the resulting ToE_{ts} estimates. Decadal variability of surface ocean carbon is poorly quantified by observations in general (Keller et al., 2012; McKinley et al., 2011; Schuster and Watson, 2007; Séférian et al., 2013). In the absence of constraint of decadal variability at each of these locations, we consider an example in the tropical Pacific to estimate the impact of decadal variability on ToE_{ts} . For this example, we estimate that decadal-scale forcing leads to a 27% change in surface seawater $p\text{CO}_2$ in the tropical Pacific (Feely et al. 2006) and determine the impact that added decadal variability has to the ToE estimates at the 7 sites on the Tropical Atmosphere Ocean (TAO) array. This is done by repeating the existing $p\text{CO}_2$ time series until time series length is 50 years and applying a +27% offset in the data on 10-year intervals at random. This simulated 50-year time series is then used to recalculate ToE . The simulation with added low-frequency decadal signals increases ToE by an average of 40% across the TAO sites. Decadal forcing has less impact in the eastern Pacific where sub-seasonal to interannual variability controlled by equatorial upwelling, tropical instability waves, and biological productivity is dominant, and more impact in the central and western Pacific where these higher-frequency modes of variability are less pronounced.

Decadal forcing may be particularly strong in the tropical Pacific (Feely et al., 2006; Sutton et al., 2014a) compared to other subtropical sites (Keller et al., 2012; Landschützer et al., 2016; Lovenduski et al., 2015; Schuster and Watson, 2007). However, we apply this 40% increase in ToE_{ts} to the time series from other regions in order to provide a conservative estimate of when an anthropogenic signal can be detected using these moored time series data. The reported ToE for each moored time series is the result from Eq. (1) multiplied by 1.4:

$$\text{ToE} = \text{ToE}_{\text{ts}} \times 1.4 \quad (4)$$

For the data sets with time series length greater than these ToE estimates, monthly anomalies are linearly regressed against time to determine the long-term rate of change. Linear regression statistics, including uncertainty in rate and r^2 , are calculated using standard methods described in Glover et al. (2011).

3 Results and Discussion

3.1 Climatology and natural variability

Across the 40 moored stations, climatological means of surface ocean $p\text{CO}_2$ range from 255 to 490 μatm (Fig. 1). Seasonal amplitude of seawater $p\text{CO}_2$ vary from 8 to 337 μatm . With more recent establishment of seawater pH observations, only 10 of the 17 sites with pH sensors have seasonally-distributed pH data necessary to determine climatological mean and seasonal amplitude. At these locations, climatological mean and seasonal amplitude of seawater pH vary from 8.00 to 8.21 and 0.01 to 0.14, respectively (Fig. 2). All the sites with seasonal amplitude reported in Figs. 1 and 2 have observations distributed across all seasons (Fig. 3). Seasonal amplitude of surface seawater $p\text{CO}_2$ is largest at the coastal sites (60 to 337 μatm) compared to the open ocean (8 to 226 μatm) and coral reef sites (11 to 178 μatm). These patterns hold for pH as well with ranges of 0.08 to 0.14, 0.01 to 0.07, and 0.02 to 0.07 at the coastal, open ocean, and coral sites, respectively.



IAV of seawater $p\text{CO}_2$, which is the standard deviation of yearly means, range from 2 to 29 μatm . The largest IAV is found at the coastal and coral sites with Coastal MS, Twanoh, and CRIMP2 IAV of 29, 27, and 25 μatm , respectively. CRIMP2 tends to be an anomaly among coral sites, however, with most tropical coral locations exhibiting IAV ≤ 5 , which is similar to IAV at the open ocean sites. Surface seawater pH time series are not yet long enough to determine a robust estimate of IAV.

- 5 These descriptive statistics show higher seawater $p\text{CO}_2$ values throughout the year in the tropical Pacific where equatorial upwelling of CO_2 -rich water dominates. Seasonal forcing of $p\text{CO}_2$ values in this region is low, but IAV, driven by the El Niño Southern Oscillation (Feely et al., 2006), is the highest of open ocean time series stations (Fig. 1). The coastal time series stations suggest annual CO_2 uptake with climatological seawater $p\text{CO}_2$ means less than atmospheric CO_2 levels. Seasonal changes of SST and biological productivity drive the large seasonal amplitudes in $p\text{CO}_2$ and pH at the U.S. coastal locations (Fassbender et al.,
- 10 2018; Reimer et al., 2017; Sutton et al., 2016; Xue et al., 2016). The coastal stations Twanoh and Coastal MS exhibit the highest IAV of seawater $p\text{CO}_2$ (reported as seawater $x\text{CO}_2$ for Twanoh) due to large variability from year to year in freshwater input and biological productivity (Fig. 1). Most coral reef time series stations suggest net annual calcification with positive $\Delta p\text{CO}_2$ (seawater – air) values. Net calcification has been confirmed by independent assessments at some of these time series stations (Bates et al., 2010; Courtney et al., 2016; Drupp et al., 2011; Shamberger et al., 2011).
- 15 Clusters of fixed time series stations in Washington State waters, the Hawaiian Island of Oahu, and Bermuda provide examples of how different processes drive ocean carbon chemistry. Seasonal variability and IAV are almost twice as large at the time series stations within the freshwater-influenced Puget Sound (Dabob and Twanoh) compared to the stations on the outer coast of Washington (Chá bã and Cape Elizabeth). Dabob is closer to the inlet of Puget Sound compared to Twanoh, which experiences greater water residence time and, therefore, greater influence of biological production and respiration on seawater $x\text{CO}_2$
- 20 (Fassbender et al., 2018; Lindquist et al., 2017). These processes can cause subsurface hypoxia and low pH (<7.4) and aragonite saturation (<0.6) conditions in this region of Puget Sound (Feely et al., 2010), which likely contribute to the elevated surface seawater $x\text{CO}_2$ levels observed at Dabob and Twanoh.

In both Hawaii and Bermuda, coral reef time series stations are paired with offshore, open ocean $p\text{CO}_2$ observatories. In both cases, the offshore stations of WHOTS and BTM both exhibit climatological mean seawater $p\text{CO}_2$ slightly below atmospheric values

25 (Fig. 1), with previous studies indicating these locations are net annual CO_2 sinks (Bates et al., 2014; Dore et al., 2009, 2003; Sutton et al., 2017). The barrier reef sites in Oahu (Kilo Nalu, Ala Wai, Kaneohe) tend to exhibit seawater $p\text{CO}_2$ values closer to these open ocean background levels. The lagoonal reefs (Crescent Reef in Bermuda and CRIMP1 and CRIMP2 in Oahu) where increased water retention time paired with coral reef photosynthesis/respiration and calcification/dissolution elevate both annual mean and daily to interannual variability in seawater $p\text{CO}_2$ values (Fig. 1; Courtney et al. 2017; Drupp et al. 2011). One exception

30 is the equally as large IAV at the barrier reef Ala Wai site, which is impacted by a nearby urban canal with high nutrient and organic matter input during storm events (Drupp et al., 2013). Positive $\Delta p\text{CO}_2$ values at the lagoonal reef sites also suggest these sites are a net source of CO_2 to the atmosphere in contrast to the annual net CO_2 uptake at the nearby open ocean sites.

3.2 Marine boundary layer atmospheric CO_2

Atmospheric CO_2 observations at the 40 time series sites all show a positive long-term trend (Fig. 4a). The mean trend at the open

35 ocean sites are not significantly different from the global average rate of change of 2 ppm yr^{-1} (Sutton et al., 2014b). Fig. 4a shows all 40 time series of atmospheric $x\text{CO}_2$ with a rate of change of approximately 20 $\mu\text{mol mol}^{-1}$ (or ppm) over a decade: from 380 $\mu\text{mol mol}^{-1}$ in January 2006 to 400 $\mu\text{mol mol}^{-1}$ in January 2016.



Although the global observing network of atmospheric CO₂ that tracks anthropogenic CO₂ increase requires higher measurement quality (≤ 0.1 ppm) compared to the measurement quality of the MAPCO₂ system (≤ 1 ppm), the MAPCO₂ air data may be valuable for regional air CO₂ studies in coastal regions where land-based activities cause larger hourly to interannual noise in atmospheric CO₂ (Bender et al., 2002). In general, the coastal stations exhibit higher annual means and seasonal amplitude compared to GLOBALVIEW-CO₂ MBL values, which is a product based on interpolating high-quality atmospheric measurements around the globe to latitudinal distributions of biweekly CO₂ (Fig. 4b,c). Open ocean and coral reefs sites do not show this overall pattern compared to GLOBALVIEW-CO₂ MBL values, although there is variability across the sites with some time series exhibiting higher means and seasonal amplitudes compared to the data product and vice versa (Fig. 4b,c).

3.3 Emergence of anthropogenic trends in surface seawater $p\text{CO}_2$ and pH

- 10 Estimated length of time for an anthropogenic trend in seawater $p\text{CO}_2$ to emerge from natural variability in the 40 time series varies from 8 to 41 years (Fig. 5). This range is 8-15 years at the open ocean sites, 16-41 years at the coastal sites, and 9-22 years at the coral reef sites. For the pH data sets with long enough time series to calculate ToE (i.e., the circles in Fig. 2), there is no significant difference between ToE of $p\text{CO}_2$ and pH, therefore, it is likely that ToE presented in Fig. 5 signifies both surface seawater $p\text{CO}_2$ and pH.
- 15 Since ToE is dependent on the noise in the data, the sites that exhibit higher variability (Figs. 1 and 2) tend to have longer ToE estimates. The barrier reef sites of south shore Oahu (Kilo Nalu and Ala Wai) and Kaneohe Bay have shorter ToE compared to the lagoonal sites (CRIMP1 and CRIMP2) with larger seasonal to interannual noise. Similarly, the freshwater-influenced, highly-productive Puget Sound sites (Dabob and Twanoh) have the longest ToE of all 40 sites and are approximately twice as long as the nearby time series on the outer coast of Washington (Chá bã and Cape Elizabeth).
- 20 These data also suggest that removing seasonal variability from the times series is essential to reducing ToE and determining accurate long-term trends. The ToE estimates presented in Fig. 5 are based on deseasoned monthly anomalies, which are the residuals of the climatological monthly means. These ToE estimates are on average 55% shorter than ToE estimates based on the raw time series data. This reduction in ToE due to deseasoning has a larger impact at higher latitudes where the seasonal amplitude of surface seawater $p\text{CO}_2$ is larger compared to tropical sites. Using anomalies of climatological monthly means also minimizes
- 25 the impact of start and end month of the time series on the resulting trend estimation.

Of the 40 seawater $p\text{CO}_2$ time series, ToE estimates suggest only the WHOTS and Stratus time series are currently long enough to detect an anthropogenic trend. These data suggest the anthropogenic trend in surface seawater $p\text{CO}_2$ at WHOTS from 2004-2014 is $1.9 \pm 0.3 \mu\text{atm yr}^{-1}$ (Fig. 6). In this trend analysis we do not include data from the 2014-2015 anomalous event that warmed North Pacific surface water (Bond et al., 2015; Feely et al., 2017) and elevated seawater $p\text{CO}_2$ values. This WHOTS trend is not significantly different from the seawater $p\text{CO}_2$ trend observed from 1988 to 2013 at the collocated Station ALOHA of $2.0 \pm 0.1 \mu\text{atm yr}^{-1}$ (Sutton et al., 2017). Both WHOTS and Station ALOHA trends are not significantly different from the trend expected if surface seawater was in equilibrium with the global average atmospheric CO₂ increase.

The long-term trend at Stratus from 2006-2015 is $1.6 \pm 0.3 \mu\text{atm yr}^{-1}$ (Fig. 6). This trend is slightly lower than expected if seawater $p\text{CO}_2$ change is in equilibrium with the atmosphere. Considering the uncertainty in the ToE_{is} estimate (Table 2) and the added uncertainty around unconstrained decadal variability at each of these locations, continued observations will be necessary at this site to confirm whether this lower rate of change persists. In addition to uptake of atmospheric CO₂, the seawater $p\text{CO}_2$ trend may be impacted by surface meteorological or upper ocean changes in this region. Significant trends in wind speed, wind stress, and the air-sea exchange of heat, freshwater, and momentum were observed from meteorological and surface ocean measurements on



Stratus from 2000 to 2009. These observations suggest a decadal-scale or longer-term change in southeast trade winds in the South Pacific (Weller, 2015). This is a region where a sustained, continuous Stratus time series can contribute to constraining the physical and biogeochemical processes controlling long-term change.

4 Data Availability

- 5 Locations of deployment-level archived data at NCEI and the time series data product for each mooring site are listed in Table 2. The Digital Object Identifier (DOI) for this data product is:10.7289/V5DB8043. Data users looking for easier access to quality-assured seawater $p\text{CO}_2$ and pH data designated good (QF = 2; see Sect. 2.2) should consider using this time series data product. The time series data files will be updated each time new deployment-level data are submitted to the NCEI archive. Data users interested in all available MAPCO₂ and pH data should retrieve deployment-level data at NCEI (links also provided in Table 2).
- 10 These data are made freely available to the public and the scientific community in the belief that their wide dissemination will lead to greater understanding and new scientific insights. Users of these time series data products should reference this paper and acknowledge the major funding organizations of this work: NOAA's Ocean Observing and Monitoring Division and Ocean Acidification Program. Manuscripts using the time series data should be sent to the data provider for review before submission to ensure that the quality and limitations of the data are accurately represented. If the time series data are essential to the work or if
- 15 an important result or conclusion depends on the data, co-authorship may be appropriate.

5 Conclusions

- This product provides a unique data set for a range of users, including providing a more accessible format for non-carbon chemists interested in surface ocean $p\text{CO}_2$ and pH time series data. These 40 time series locations represent a range of ocean, coastal, and coral reef regimes that exhibit a broad spectrum of daily to interannual variability. These time series can be used as a tool for
- 20 assessing climatology and natural variability in these regions. However, at this time, only two time series data sets are long enough (WHOTS and Stratus) to estimate long-term anthropogenic trends. ToE estimates show at all but these two sites, an anthropogenic signal cannot be discerned at a statistically significant level from the noise inherent in the natural variability of surface seawater $p\text{CO}_2$ and pH. If and when that date of trend emergence is attained, it is essential to deseason data prior to any trend analyses. Even though the ToE provided are conservative estimates, data users should still use caution in interpreting that an anthropogenic trend
 - 25 is distinct from decadal-scale ocean forcing that is not well characterized. Future work should be directed at improving upon these ToE estimates in regions where other data, proxies, or knowledge about decadal forcing are more complete.

Acknowledgements

- We gratefully acknowledge the major funders of the $p\text{CO}_2$ and pH observations: the Office of Oceanic and Atmospheric Research of the National Oceanic and Atmospheric Administration, U.S. Department of Commerce, including resources from the Ocean
- 30 Observing and Monitoring Division of the Climate Program Office (fund reference number 100007298) and the Ocean Acidification Program. We rely on a long list of partners and their technical staff who carry out buoy maintenance, sensor deployment, and ancillary measurements at sea including: Uwe Send and Mark Ohman (CCE), Meghan Cronin (Papa, KEO, and JKEO), Robert Weller (WHOTS and Stratus), National Data Buoy Center (TAO and Cape Elizabeth), Nick Bates (BTM), Solveig Olafsdottir and Jon Olafsson (Iceland), Mike McPhaden (BOBOA), Tom Trull (SOFS), Jan Newton and John Mickett (Chá bã,
 - 35 Dabob, and Twanoh), Burke Hales (NH-10), Eric DeCarlo (Ala Wai, Kilo Nalu, Kaneohe, and CRIMP), Jae-Hoon Noh and Charity



Lee (Chuuk), Wei-Jun Cai and Scott Noakes (Gray's Reef), Joseph Salisbury and Doug Vandemark (Gulf of Maine), Andreas Andersson (Hog Reef and Crescent Reef), Stephan Howden (Coastal MS), Derek Manzello (Cheeca Rocks), and Julio Morell (La Parguera). We thank these partners and their funders for their continued efforts in sustaining the platforms that support these long-term $p\text{CO}_2$ and pH observations. This paper is PMEL contribution number 4797.

5 References

- Bakker, D. C. E., Pfeil, B., Landa, C. S., Metzl, N., O'Brien, K. M., Olsen, A., Smith, K., Cosca, C., Harasawa, S., Jones, S. D., Nakaoka, S. I., Nojiri, Y., Schuster, U., Steinhoff, T., Sweeney, C., Takahashi, T., Tilbrook, B., Wada, C., Wanninkhof, R., Alin, S. R., Balestrini, C. F., Barbero, L., Bates, N. R., Bianchi, A. A., Bonou, F., Boutin, J., Bozec, Y., Burger, E. F., Cai, W. J., Castle, R. D., Chen, L., Chierici, M., Currie, K., Evans, W., Featherstone, C., Feely, R. A., Fransson, A., Goyet, C., Greenwood, N.,
- 10 Gregor, L., Hankin, S., Hardman-Mountford, N. J., Harlay, J., Hauck, J., Hoppema, M., Humphreys, M. P., Hunt, C. W., Huss, B., Ibáñez, J. S. P., Johannessen, T., Keeling, R., Kitidis, V., Körtzinger, A., Kozyr, A., Krasakopoulou, E., Kuwata, A., Landschützer, P., Lauvset, S. K., Lefèvre, N., Lo Monaco, C., Manke, A., Mathis, J. T., Merlivat, L., Millero, F. J., Monteiro, P. M. S., Munro, D. R., Murata, A., Newberger, T., Omar, A. M., Ono, T., Paterson, K., Pearce, D., Pierrot, D., Robbins, L. L., Saito, S., Salisbury, J., Schlitzer, R., Schneider, B., Schweitzer, R., Sieger, R., Skjelvan, I., Sullivan, K. F., Sutherland, S. C., Sutton, A.
- 15 J., Tadokoro, K., Telszewski, M., Tuma, M., van Heuven, S. M. A. C., Vandemark, D., Ward, B., Watson, A. J., and Xu, S.: A multi-decade record of high-quality $f\text{CO}_2$ data in version 3 of the Surface Ocean CO_2 Atlas (SOCAT), *Earth Syst. Sci. Data*, 8, 383–413, doi:10.5194/essd-8-383-2016, 2016.
- Barton, A., Hales, B., Waldbusser, G. G., Langdon, C., and Feely, R. A.: The Pacific oyster, *Crassostrea gigas*, shows negative correlation to naturally elevated carbon dioxide levels: Implications for near-term ocean acidification effects, *Limnol. Oceanogr.*,
- 20 57, 698–710, doi:10.4319/lo.2012.57.3.0698, 2012.
- Barton, A., Waldbusser, G. G., Feely, R. A., Weisberg, S. B., Newton, J. A., Hales, B., Cudd, S., Eudeline, B., Langdon, C. J., Jefferds, I., King, T., Suhrbier, A., and McLaughlin, K.: Impacts of coastal acidification on the Pacific Northwest shellfish industry and adaptation strategies implemented in response, *Oceanography*, 28, 146–159, doi:10.5670/oceanog.2015.38, 2015.
- Bates, N. R.: Interannual variability of oceanic CO_2 and biogeochemical properties in the western North Atlantic subtropical gyre,
- 25 *Deep-Sea Res. Pt. II*, 48, 1507–1528, 2001.
- Bates, N. R., Amat, A., and Andersson, A. J.: Feedbacks and responses of coral calcification on the Bermuda reef system to seasonal changes in biological processes and ocean acidification, *Biogeosciences*, 7, 2509–2530, doi:10.5194/bg-7-2509-2010, 2010.
- Bates, N. R., Astor, Y. M., Church, M. J., Currie, K., Dore, J. E., González-Dávila, M., Lorenzoni, L., Muller-Karger, F., Olafsson,
- 30 J., and Santana-Casiano, J. M.: A time-series view of changing ocean chemistry due to ocean uptake of anthropogenic CO_2 and ocean acidification, *Oceanography*, 27, 126–141, doi:10.5670/oceanog.2014.16, 2014.
- Bauer, J. E., Cai, W.-J., Raymond, P. A., Bianchi, T. S., Hopkinson, C. S., and Regnier, P. A. G.: The changing carbon cycle of the coastal ocean, *Nature*, 504, 61–70, doi:10.1038/nature12857, 2013.
- Bednaršek, N., Tarling, G. A., Bakker, D. C. E., Fielding, S., and Feely, R. A.: Dissolution dominating calcification process in
- 35 polar pteropods close to the point of aragonite undersaturation, *PLoS ONE*, 9, e109183, doi:10.1371/journal.pone.0109183, 2014.



- Bednaršek, N., Harvey, C. J., Kaplan, I. C., Feely, R. A., and Možina, J.: Pteropods on the edge: Cumulative effects of ocean acidification, warming, and deoxygenation, *Prog. Oceanogr.*, 145, 1–24, doi:10.1016/j.pocean.2016.04.002, 2016.
- Bednaršek, N., Feely, R. A., Tolimieri, N., Hermann, A. J., Siedlecki, S. A., Waldbusser, G. G., McElhany, P., Alin, S. R., Klinger, T., Moore-Maley, B., and Pörtner, H. O.: Exposure history determines pteropod vulnerability to ocean acidification along the US West Coast, *Sci. Rep.*, 7, 4526, doi:10.1038/s41598-017-03934-z, 2017a.
- Bednaršek, N., Klinger, T., Harvey, C. J., Weisberg, S., McCabe, R. M., Feely, R. A., Newton, J., and Tolimieri, N.: New ocean, new needs: Application of pteropod shell dissolution as a biological indicator for marine resource management, *Ecol. Indic.*, 76, 240–244, doi:10.1016/j.ecolind.2017.01.025, 2017b.
- Bender, M., Doney, S., Feely, R. A., Fung, I. Y., Gruber, N., Harrison, D. E., Keeling, R., Moore, J., Sarmiento, J., Sarachik, E., Stephens, B., Takahashi, T., Tans, P. P., and Wanninkhof, R.: A Large Scale Carbon Observing Plan: In Situ Oceans and Atmosphere (LSCOP), *Nat. Tech. Info. Service*, Springfield, 201 pp., 2002.
- Bond, N. A., Cronin, M. F., Freeland, H., and Mantua, N.: Causes and impacts of the 2014 warm anomaly in the NE Pacific, *Geophys. Res. Lett.*, 42, 3414–3420. doi:10.1002/2015GL063306, 2015.
- Bresnahan, P. J., Martz, T. R., Takeshita, Y., Johnson, K. S., and LaShomb, M.: Best practices for autonomous measurement of seawater pH with the Honeywell Durafet, *Method. Oceanogr.*, 9, 44–60, doi:10.1016/j.mio.2014.08.003, 2014.
- Courtney, T. A., Andersson, A. J., Bates, N. R., Collins, A., Cyronak, T., de Putron, S. J., Eyre, B. D., Garley, R., Hochberg, E. J., Johnson, R., Musielewicz, S., Noyes, T. J., Sabine, C. L., Sutton, A. J., Toncin, J., and Tribollet, A.: Comparing chemistry and census-based estimates of net ecosystem calcification on a rim reef in Bermuda, *Front. Mar. Sci.*, 3, 181, doi:10.3389/fmars.2016.00181, 2016.
- Courtney, T. A., Lebrato, M., Bates, N. R., Collins, A., de Putron, S. J., Garley, R., Johnson, R., Molinero, J.-C., Noyes, T. J., Sabine, C. L., and Andersson, A. J.: Environmental controls on modern scleractinian coral and reef-scale calcification, *Sci. Adv.*, 3, e1701356, doi:10.1126/sciadv.1701356, 2017.
- Davis, C. V., Rivest, E. B., Hill, T. M., Gaylord, B., Russell, A. D., and Sanford, E.: Ocean acidification compromises a planktic calcifier with implications for global carbon cycling, *Sci. Rep.*, 7, 2225, doi:10.1038/s41598-017-01530-9, 2017.
- Dickson, A. G., Sabine, C. L., and Christian, J. R.: Guide to Best Practices for Ocean CO₂ Measurements. North Pacific Marine Science Organization, 176 pp., 2007.
- Dore, J. E., Lukas, R., Sadler, D. W., and Karl, D. M.: Climate-driven changes to the atmospheric CO₂ sink in the subtropical North Pacific Ocean, *Nature*, 424, 754–757, 2003.
- Dore, J. E., Lukas, R., Sadler, D. W., Church, M. J., and Karl, D. M.: Physical and biogeochemical modulation of ocean acidification in the central North Pacific, *Proc. Natl. Acad. Sci.*, 106, 12235–12240, 2009.
- Drupp, P., De Carlo, E. H., Mackenzie, F. T., Bienfang, P., and Sabine, C. L.: Nutrient inputs, phytoplankton response, and CO₂ variations in a semi-enclosed subtropical embayment, Kaneohe Bay, Hawaii, *Aquat. Geochem.*, 17, 473–498, doi:10.1007/s10498-010-9115-y, 2011.
- Drupp, P. S., De Carlo, E. H., Mackenzie, F. T., Sabine, C. L., Feely, R. A., and Shamberger, K. E.: Comparison of CO₂ dynamics and air-sea gas exchange in differing tropical reef environments, *Aquat. Geochem.*, 19, 371–397, doi:10.1007/s10498-013-9214-7, 2013.



- Eyre, B. D., Cyronak, T., Drupp, P., De Carlo, E. H., Sachs, J. P., and Andersson, A. J.: Coral reefs will transition to net dissolving before end of century, *Science*, 359, 908–911, doi:10.1126/science.aao1118, 2018.
- Fassbender, A. J., Alin, S. R., Feely, R. A., Sutton, A. J., Newton, J. A., Krembs, C., Bos, J., Keyzers, M., Devol, A., Ruef, W., and Pelletier, G.: Seasonal carbonate chemistry variability in marine surface waters of the Pacific Northwest, *Earth Syst. Sci. Data Discuss.*, doi:10.5194/essd-2017-138, 2018.
- 5 Feely, R. A., Alin, S. R., Newton, J., Sabine, C. L., Warner, M., Devol, A., Krembs, C., and Maloy, C.: The combined effects of ocean acidification, mixing, and respiration on pH and carbonate saturation in an urbanized estuary, *Estuar. Coast. Shelf Sci.*, 88, 442–449, doi:10.1016/j.ecss.2010.05.004, 2010.
- Feely, R. A., Takahashi, T., Wanninkhof, R., McPhaden, M. J., Cosca, C. E., Sutherland, S. C., and Carr, M.-E.: Decadal variability of the air-sea CO₂ fluxes in the equatorial Pacific Ocean, *J. Geophys. Res.*, 111, C08S90, doi:10.1029/2005JC003129, 2006.
- 10 Feely, R. A., Wanninkhof, R., Landschützer, P., Carter, B. R., and Triñanes, J. A.: Ocean carbon. In *State of the Climate in 2016*, Global Oceans, *Bull. Am. Meteorol. Soc.*, 98, S89–S92, 2017.
- Gattuso, J.-P., Magnan, A., Billé, R., Cheung, W. W. L., Howes, E. L., Joos, F., Allemand, D., Bopp, L., Cooley, S. R., Eakin, C. M., Hoegh-Guldberg, O., Kelly, R. P., Pörtner, H.-O., Rogers, A. D., Baxter, J. M., Laffoley, D., Osborn, D., Rankovic, A., Rochette, J., Sumaila, U. R., Treyer, S., and Turley, C.: Contrasting futures for ocean and society from different anthropogenic CO₂ emissions scenarios, *Science*, 349, aac4722, doi:10.1126/science.aac4722, 2015.
- 15 GLOBALVIEW-CO₂: Cooperative Global Atmospheric Data Integration Project: Multilaboratory compilation of synchronized and gap-filled atmospheric carbon dioxide records for the period 1979–2012 (obspack_co2_1_GLOBALVIEW-CO₂_2013_v1.0.4_2013-12-23), compiled by NOAA Global Monitoring Division: Boulder, Colorado, USA Data product accessed at: doi:10.3334/OBSPACK/1002, 2013 (updated annually).
- 20 Glover, D. M., Jenkins, W. J., and Doney, S. C.: *Modeling Methods for Marine Science*. Cambridge University Press, New York, 2011.
- Henson, S. A., Sarmiento, J. L., Dunne, J. P., Bopp, L., Lima, I., Doney, S. C., John, J., and Beaulieu, C.: Detection of anthropogenic climate change in satellite records of ocean chlorophyll and productivity, *Biogeosciences*, 7, 621–640, doi:10.5194/bg-7-621-2010, 2010.
- 25 Hofmann, G. E., Barry, J. P., Edmunds, P. J., Gates, R. D., Hutchins, D. A., Klinger, T., and Sewell, M. A.: The effect of ocean acidification on calcifying organisms in marine ecosystems: An organism-to-ecosystem perspective, *Annu. Rev. Ecol. Evol. Syst.*, 41, 127–147, doi:10.1146/annurev.ecolsys.110308.120227, 2010.
- Keller, K. M., Joos, F., Raible, C. C., Cocco, V., Frölicher, T. L., Dunne, J. P., Gehlen, M., Bopp, L., Orr, J. C., Tjiputra, J., Heinze, C., Segsneider, J., Roy, T., and Metzl, N.: Variability of the ocean carbon cycle in response to the North Atlantic Oscillation, *Tellus B*, 64, 18738, doi:10.3402/tellusb.v64i0.18738, 2012.
- 30 Khatiwala, S., Tanhua, T., Mikaloff Fletcher, S., Gerber, M., Doney, S. C., Graven, H. D., Gruber, N., McKinley, G. A., Murata, A., Ríos, A. F., Sabine, C. L., and Sarmiento, J. L.: Global ocean storage of anthropogenic carbon, *Biogeosciences*, 10, 2169–2191, doi:10.5194/bg-10-2169-2013, 2013.
- 35 Landschützer, P., Gruber, N., and Bakker, D. C. E.: Decadal variations and trends of the global ocean carbon sink, *Global Biogeochem. Cy.*, 30, 1396–1417, doi:10.1002/2015GB005359, 2016.



- Le Quéré, C., Andrew, R. M., Friedlingstein, P., Sitch, S., Pongratz, J., Manning, A. C., Korsbakken, J. I., Peters, G. P., Canadell, J. G., Jackson, R. B., Boden, T. A., Tans, P. P., Andrews, O. D., Arora, V. K., Bakker, D. C. E., Barbero, L., Becker, M., Betts, R. A., Bopp, L., Chevallier, F., Chini, L. P., Ciais, P., Cosca, C. E., Cross, J., Currie, K., Gasser, T., Harris, I., Hauck, J., Haverd, V., Houghton, R. A., Hunt, C. W., Hurtt, G., Ilyina, T., Jain, A. K., Kato, E., Kautz, M., Keeling, R. F., Klein Goldewijk, K.,
- 5 Körtzinger, A., Landschützer, P., Lefèvre, N., Lenton, A., Lienert, S., Lima, I., Lombardozi, D., Metzl, N., Millero, F., Monteiro, P. M. S., Munro, D. R., Nabel, J. E. M. S., Nakaoka, S. I., Nojiri, Y., Padin, X. A., Peregon, A., Pfeil, B., Pierrot, D., Poulter, B., Rehder, G., Reimer, J., Rödenbeck, C., Schwinger, J., Séférian, R., Skjelvan, I., Stocker, B. D., Tian, H., Tilbrook, B., Tubiello, F. N., van der Laan-Luijkx, I. T., van der Werf, G. R., van Heuven, S., Viovy, N., Vuichard, N., Walker, A. P., Watson, A. J., Wiltshire, A. J., Zaehle, S., and Zhu, D.: Global Carbon Budget 2017, *Earth Syst. Sci. Data*, 10, 405–448, doi:10.5194/essd-10-10 405-2018, 2018.
- Lindquist, A., Sutton, A., Devol, A., Winans, A., Coyne, A., Bodenstein, B., Curry, B., Herrmann, B., Sackmann, B., Tyler, B., Maloy, C., Greengrove, C., Fanshier, C., Krembs, C., Sabine, C., Cook, C., Hard, C., Greene, C., Lowry, D., Harvell, D., McPhee-Shaw, E., Haphey, E., Hannach, G., Bohlmann, H., Burgess, H., Smith, I., Kemp, I., Newton, J., Borchert, J., Mickett, J., Apple, J., Bos, J., Parrish, J., Ruffner, J., Keister, J., Masura, J., Devitt, K., Bumbaco, K., Stark, K., Hermanson, L., Claassen, L., Swanson,
- 15 L., Burger, M., Schmidt, M., McCartha, M., Peacock, M., Eisenlord, M., Keyzers, M., Christman, N., Hamel, N., Burnett, N., Bond, N., Graham, O., Biondo, P., Hodum, P., Wilborn, R., Feely, R. A., Pearson, S., Alin, S., Albertson, S., Moore, S., Jaeger, S., Pool, S., Musielwicz, S., King, T., Good, T., Jones, T., Ross, T., Sandell, T., Burks, T., Trainer, V., Bowes, V., Ruef, W., and Eash-Loucks, W.: Puget Sound Marine Waters: 2016 Overview, edited by: Moore, S., Wold, R., Stark, K., Bos, J., Williams, P., Hamel, N., Edwards, A., Krembs, C., and Newton, J. NOAA Northwest Fisheries Science Center for the Puget Sound Ecosystem
- 20 Monitoring Program's (PSEMP) Marine Waters Workgroup, 2017.
- Lovenduski, N. S., Long, M. C., and Lindsay, K.: Natural variability in the surface ocean carbonate ion concentration, *Biogeosciences*, 12, 6321–6335, doi:10.5194/bg-12-6321-2015, 2015.
- Martz, T. R., Connery, J. G., and Johnson, K. S.: Testing the Honeywell Durafet® for seawater pH applications, *Limnol. Oceanogr. Methods*, 8, 172–184, doi:10.4319/lom.2010.8.172, 2010.
- 25 McKinley, G. A., Fay, A. R., Takahashi, T., and Metzl, N.: Convergence of atmospheric and North Atlantic carbon dioxide trends on multidecadal timescales, *Nat. Geosci.*, 4, 606–610, doi:10.1038/ngeo1193, 2011.
- Reimer, J. J., Cai, W.-J., Xue, L., Vargas, R., Noakes, S., Hu, X., Signorini, S. R., Mathis, J. T., Feely, R. A., Sutton, A. J., Sabine, C., Musielewicz, S., Chen, B., and Wanninkhof, R.: Time series $p\text{CO}_2$ at a coastal mooring: Internal consistency, seasonal cycles, and interannual variability, *Cont. Shelf Res.*, 145, 95–108, doi:10.1016/j.csr.2017.06.022, 2017.
- 30 Reum, J. C. P., Alin, S. R., Harvey, C. J., Bednaršek, N., Evans, W., Feely, R. A., Hales, B., Lucey, N., Mathis, J. T., McElhany, P., Newton, J., and Sabine, C. L.: Interpretation and design of ocean acidification experiments in upwelling systems in the context of carbonate chemistry co-variation with temperature and oxygen, *ICES J. Mar. Sci.*, 73, 582–595, doi:10.1093/icesjms/fsu231, 2015.
- Schuster, U. and Watson, A. J.: A variable and decreasing sink for atmospheric CO_2 in the North Atlantic, *J. Geophys. Res.-*
- 35 *Oceans*, 112, C11006, doi:10.1029/2006JC003941, 2007.
- Séférian, R., Bopp, L., Swingedouw, D., and Servonnat, J.: Dynamical and biogeochemical control on the decadal variability of ocean carbon fluxes, *Earth Syst. Dynam.*, 4, 109–127, doi:10.5194/esd-4-109-2013, 2013.



- Seidel, M. P., DeGrandpre, M. D., and Dickson, A. G.: A sensor for in situ indicator-based measurements of seawater pH, *Mar. Chem.*, 109, 18–28, 2008.
- Shamberger, K. E. F., Feely, R. A., Sabine, C. L., Atkinson, M. J., DeCarlo, E. H., Mackenzie, F. T., Drupp, P. S., and Butterfield, D. A.: Calcification and organic production on a Hawaiian coral reef, *Mar. Chem.*, 127, 64–75, doi:10.1016/j.marchem.2011.08.003, 2011.
- 5 Sutton, A. J., Feely, R. A., Sabine, C. L., McPhaden, M. J., Takahashi, T., Chavez, F. P., Friederich, G. E., and Mathis, J. T.: Natural variability and anthropogenic change in equatorial Pacific surface ocean $p\text{CO}_2$ and pH, *Global Biogeochem. Cy.*, 28, 131–145, doi:10.1002/2013GB004679, 2014a.
- Sutton, A. J., Sabine, C. L., Feely, R. A., Cai, W. J., Cronin, M. F., McPhaden, M. J., Morell, J. M., Newton, J. A., Noh, J. H., Ólafsdóttir, S. R., Salisbury, J. E., Send, U., Vandemark, D. C., and Weller, R. A.: Using present-day observations to detect when anthropogenic change forces surface ocean carbonate chemistry outside preindustrial bounds, *Biogeosciences*, 13, 5065–5083, doi:10.5194/bg-13-5065-2016, 2016.
- 10 Sutton, A. J., Sabine, C. L., Maenner-Jones, S., Lawrence-Slavas, N., Meinig, C., Feely, R. A., Mathis, J. T., Musielewicz, S., Bott, R., McLain, P. D., Fought, H. J., and Kozyr, A.: A high-frequency atmospheric and seawater $p\text{CO}_2$ data set from 14 open-ocean sites using a moored autonomous system, *Earth Syst. Sci. Data*, 6, 353–366, doi:10.5194/essd-6-353-2014, 2014b.
- 15 Sutton, A. J., Wanninkhof, R., Sabine, C. L., Feely, R. A., Cronin, M. F., and Weller, R. A.: Variability and trends in surface seawater $p\text{CO}_2$ and CO_2 flux in the Pacific Ocean, *Geophys. Res. Lett.*, 44(11), 5627–5636, doi:10.1002/2017GL073814, 2017.
- Takahashi, T., Sutherland, S. C., Wanninkhof, R., Sweeney, C., Feely, R. A., Chipman, D. W., Hales, B., Friederich, G., Chavez, F., Sabine, C., Watson, A., Bakker, D. C. E., Schuster, U., Metzl, N., Yoshikawa-Inoue, H., Ishii, M., Midorikawa, T., Nojiri, Y., Körtzinger, A., Steinhoff, T., Hoppema, M., Olafsson, J., Arnarson, T. S., Tilbrook, B., Johannessen, T., Olsen, A., Bellerby, R., Wong, C. S., Delille, B., Bates, N. R., and de Baar, H. J. W.: Climatological mean and decadal change in surface ocean $p\text{CO}_2$, and net sea-air CO_2 flux over the global oceans, *Deep-Sea Res. Pt. II*, 56, 554–577, 2009.
- 20 Wanninkhof, R., Park, G.-H., Takahashi, T., Sweeney, C., Feely, R., Nojiri, Y., Gruber, N., Doney, S. C., McKinley, G. A., Lenton, A., Le Quéré, C., Heinze, C., Schwinger, J., Graven, H., and Khatiwala, S.: Global ocean carbon uptake: magnitude, variability and trends, *Biogeosciences*, 10, 1983–2000, doi:10.5194/bg-10-1983-2013, 2013.
- 25 Weatherhead, E. C., Reinsel, G. C., Tiao, G. C., Meng, X.-L., Choi, D., Cheang, W.-K., Keller, T., DeLuisi, J., Wuebbles, D. J., Kerr, J. B., Miller, A. J., Oltmans, S. J., and Frederick, J. E.: Factors affecting the detection of trends: Statistical considerations and applications to environmental data, *J. Geophys. Res.-Atmos.*, 103, 17149–17161, 1998.
- Weiss, R. F.: Carbon dioxide in water and seawater: the solubility of a non-ideal gas, *Mar. Chem.*, 2, 203–215, 1974.
- 30 Weller, R. A.: Variability and trends in surface meteorology and air–sea fluxes at a site off Northern Chile, *J. Climate*, 28, 3004–3023, doi:10.1175/JCLI-D-14-00591.1, 2015.
- Xue, L., Cai, W.-J., Hu, X., Sabine, C., Jones, S., Sutton, A. J., Jiang, L.-Q., and Reimer, J. J.: Sea surface carbon dioxide at the Georgia time series site (2006–2007): Air–sea flux and controlling processes, *Prog. Oceanogr.*, 140, 14–26, 2016.

**Table 1: Region, coordinates, surface ocean carbon parameters measured, year carbon time series established, and current status of the 40 fixed moored time series stations. All time series also include atmospheric CO₂, SST, and SSS.**

Abbreviation	Descriptive name	Region	Latitude	Longitude	Carbon parameters	Start year	Status
CCE1	California Current Ecosystem 1	Northeast Pacific Ocean	33.48	-122.51	pCO ₂ , pH	2008	active
Papa	Ocean Station Papa	Northeast Pacific Ocean	50.13	-144.84	pCO ₂ , pH	2007	active
KEO	Kuroshio Extension Observatory	Northwest Pacific Ocean	32.28	144.58	pCO ₂ , pH	2007	active
JKEO	Japanese Kuroshio Extension Observatory	Northwest Pacific Ocean	37.93	146.52	pCO ₂	2007	discontinued in 2007
WHOTS	Woods Hole Oceanographic Institution Hawaii Ocean Time-series Station	Central Pacific Ocean	22.67	-157.98	pCO ₂ , pH	2004 ^a	active
TAO110W	National Data Buoy Center (NDBC) Tropical Atmosphere Ocean 0°, 110°W	Equatorial Pacific Ocean	0.00	-110.00	pCO ₂	2009	active
TAO125W	NDBC Tropical Atmosphere Ocean 0°, 125°W	Equatorial Pacific Ocean	0.00	-125.00	pCO ₂	2004	active
TAO140W	NDBC Tropical Atmosphere Ocean 0°, 140°W	Equatorial Pacific Ocean	0.00	-140.00	pCO ₂	2004	active
TAO155W	NDBC Tropical Atmosphere Ocean 0°, 155°W	Equatorial Pacific Ocean	0.00	-155.00	pCO ₂	2010	active
TAO170W	NDBC Tropical Atmosphere Ocean 0°, 170°W	Equatorial Pacific Ocean	0.00	-170.00	pCO ₂	2005	active
TAO165E	NDBC Tropical Atmosphere Ocean 0°, 165°E	Equatorial Pacific Ocean	0.00	165.00	pCO ₂	2010	active
TAO8S165E	NDBC Tropical Atmosphere Ocean 8°S, 165°E	Equatorial Pacific Ocean	-8.00	165.00	pCO ₂	2009	active
Stratus	Stratus	Southeast Pacific Ocean	-19.70	-85.60	pCO ₂ , pH	2006	active
BTM	Bermuda Testbed Mooring	North Atlantic Ocean	31.50	-64.20	pCO ₂	2005	discontinued in 2007
Iceland	North Atlantic Ocean Acidification Mooring	North Atlantic Ocean	68.00	-12.67	pCO ₂ , pH	2013	active
BOBOA	Bay of Bengal Ocean Acidification Observatory	Indian Ocean	15.00	90.00	pCO ₂ , pH	2013	active
SOFS	Southern Ocean Flux Station	Southern Ocean	-46.80	142.00	pCO ₂	2011	active
GAKOA	Gulf of Alaska Ocean Acidification Mooring	Alaskan Coast	59.910	-149.350	pCO ₂ , pH ^b	2011	active
Kodiak	Kodiak Alaska Ocean Acidification Mooring	Alaskan Coast	57.700	-152.310	pCO ₂ , pH ^b	2013	discontinued in 2016
SEAK	Southeast Alaska Ocean Acidification Mooring	Alaskan Coast	56.260	134.670	pCO ₂ , pH ^b	2013	discontinued in 2016
M2	Southeastern Bering Sea Mooring Site 2	Bering Sea Coastal Shelf	56.510	-164.040	pCO ₂ , pH ^b	2013	active
Cape Elizabeth	NDBC Buoy 46041 in Olympic Coast National Marine Sanctuary (NMS)	U.S. West Coast	47.353	-124.731	pCO ₂	2006	active
Chá bá	Chá bá Buoy in the Northwest Enhanced Moored Observatory and Olympic Coast NMS	U.S. West Coast	47.936	-125.958	pCO ₂ , pH	2010	active
CCE2	California Current Ecosystem 2	U.S. West Coast	34.324	-120.814	pCO ₂ , pH	2010	active
Dabob	Oceanic Remote Chemical Analyzer (ORCA) buoy at Dabob in Hood Canal	U.S. West Coast	47.803	-122.803	xCO ₂ ^c	2011	active
NH-10	Newport Hydrographic Line Station 10 Ocean Acidification Mooring	U.S. West Coast	44.904	-124.778	pCO ₂ , pH	2014	moved to new location in 2017 ^d
Twanoh	ORCA buoy at Twanoh in Hood Canal	U.S. West Coast	47.375	-123.008	xCO ₂ ^c	2009	active
Ala Wai	Ala Wai Water Quality Buoy at South Shore Oahu	Pacific Island Coral Reef	21.280	-157.850	pCO ₂	2008	active
Chuuk	Chuuk Lagoon Ocean Acidification Mooring	Pacific Island Coral Reef	7.460	151.900	pCO ₂ , pH	2011	active
CRIMP1	Coral Reef Instrumented Monitoring Platform 1	Pacific Island Coral Reef	21.428	-157.788	pCO ₂	2005	moved to CRIMP2 in 2008
CRIMP2	Coral Reef Instrumented Monitoring Platform 2	Pacific Island Coral Reef	21.458	-157.798	pCO ₂	2008	active
Kaneohe	Kaneohe Bay Ocean Acidification Offshore Observatory	Pacific Island Coral Reef	21.480	-157.780	pCO ₂ , pH	2011	active
Kilo Nalu	Kilo Nalu Water Quality Buoy at South Shore Oahu	Pacific Island Coral Reef	21.288	-157.865	pCO ₂	2008	active
Gray's Reef	NDBC Buoy 41008 in Gray's Reef National Marine Sanctuary	U.S. East Coast	31.400	-80.870	pCO ₂ , pH	2006	active
Gulf of Maine	Coastal Western Gulf of Maine Mooring	U.S. East Coast	43.023	-70.542	pCO ₂ , pH	2006	active



Crescent Reef	Crescent Reef Bermuda Buoy	Atlantic Coral Reef	32.400	-64.790	$p\text{CO}_2$	2010	active
Hog Reef	Hog Reef Bermuda Buoy	Atlantic Coral Reef	32.460	-64.830	$p\text{CO}_2$	2010	active
Coastal MS	Central Gulf of Mexico Ocean Observing System Station 01	Gulf of Mexico Coast	30.000	-88.600	$p\text{CO}_2$, pH	2009	moved to new location in 2017 ^c
Cheeca Rocks	Cheeca Rocks Ocean Acidification Mooring in Florida Keys National Marine Sanctuary	Caribbean Coral Reef	24.910	-80.624	$p\text{CO}_2$, pH	2011	active
La Parguera	La Parguera Ocean Acidification Mooring	Caribbean Coral Reef	17.954	-67.051	$p\text{CO}_2$, pH	2009	active

Notes: ^a Data from December 2004 to July 2007 in the WHOTS time series are from the Multi-disciplinary Ocean Sensors for Environmental Analyses and Networks (MOSEAN) station at 22.80°N, 158.10°W (20 km from the WHOTS location). Previous studies have shown the MOSEAN and WHOTS locations have similar surface seawater $p\text{CO}_2$ conditions (Sutton et al., 2014b, 2017) and are therefore combined in this data product as one time series location. ^b

Measurements of pH to be included in future updates of the time series data product. ^c SST and SSS data are collected on the Dabob and Twanoh buoys at 2-hourly intervals. Because combining these data with the 3-hourly MAPCO₂ data requires making assumptions about temporal variability that reflect the research interests of the data user, only the direct measurements of CO₂ (i.e., the mole fraction of CO₂ in equilibrium with surface seawater: $x\text{CO}_2$) are available in the NCEI archived data sets. ^d The NH-10 buoy and carbon sensors were moved approximately 75 nm south to Cape Arago, Oregon: <https://www.pmel.noaa.gov/co2/story/CB-06>. ^e The Coastal MS buoy and carbon sensors were moved approximately 115 nm southwest to coastal Louisiana waters: <https://www.pmel.noaa.gov/co2/story/Coastal+LA>.



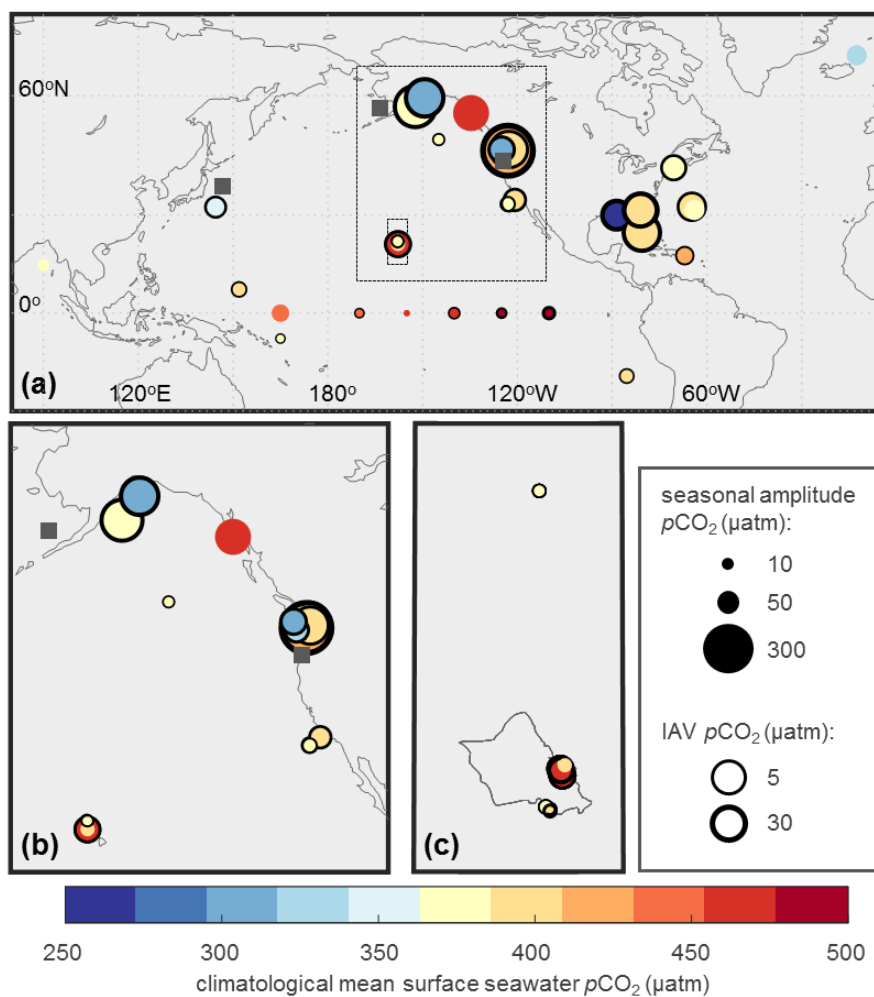
5 **Table 2: Data access to deployment-level archived data files at NCEI and the time series data product for each moored buoy location. The earliest date of seawater $p\text{CO}_2$ trend emergence is based on time series product data and calculated by adding the ToE estimate (Eqs. 1-4) to the time series start year (Table 1). The uncertainty presented here is the result of Eqs. (2-3), which is based on ToE_{ts} and does not include any additional uncertainty due to the decadal estimate from Eq. (4). NA denotes sites with less than 3 years of observations where interannual variability is likely not represented in a time series, and therefore, ToE is not calculated.**

Buoy name	NCEI archived data files (https://www.nodc.noaa.gov/...)	Time series data product (https://www.pmel.noaa.gov/co2/...)	Earliest date of seawater $p\text{CO}_2$ trend emergence
CCE1	ocads/data/0144245.xml	timeseries/CCE1.txt	2020 \pm 2
Papa	ocads/data/0100074.xml	timeseries/PAPA.txt	2017 \pm 2
KEO	ocads/data/0100071.xml	timeseries/KEO.txt	2018 \pm 2
JKEO	ocads/data/0100070.xml	timeseries/JKEO.txt	NA ^a
WHOTS	ocads/data/0100073.xml ^b ocads/data/0100080.xml	timeseries/WHOTS.txt	2013 \pm 1
TAO110W	ocads/data/0112885.xml	timeseries/TAO110W.txt	2024 \pm 4
TAO125W	ocads/data/0100076.xml	timeseries/TAO125W.txt	2017 \pm 4
TAO140W	ocads/data/0100077.xml	timeseries/TAO140W.txt	2018 \pm 2
TAO155W	ocads/data/0100084.xml	timeseries/TAO155W.txt	NA
TAO170W	ocads/data/0100078.xml	timeseries/TAO170W.txt	2016 \pm 4
TAO165E	ocads/data/0113238.xml	timeseries/TAO165E.txt	NA
TAO8S165E	ocads/data/0117073.xml	timeseries/TAO8S165E.txt	2021 \pm 2
Stratus	ocads/data/0100075.xml	timeseries/STRATUS.txt	2015 \pm 1
BTM	ocads/data/0100065.xml	timeseries/BTM.txt	NA ^a
Iceland	ocads/data/0157396.xml	timeseries/ICELAND.txt	NA
BOBOA	ocads/data/0162473.xml	timeseries/BOBOA.txt	NA
SOFS	ocads/data/0118546.xml	timeseries/SOFS.txt	NA
GAKOA	ocads/data/0116714.xml	timeseries/GAKOA.txt	2027 \pm 3
Kodiak	ocads/data/0157347.xml	timeseries/KODIAK.txt	2028 \pm 3 ^a
SEAK	ocads/data/0157601.xml	timeseries/SEAK.txt	NA ^a
M2	ocads/data/0157599.xml	timeseries/M2.txt	NA
Cape Elizabeth	ocads/data/0115322.xml	timeseries/CAPEELIZABETH.txt	2030 \pm 4
Chá bã	ocads/data/0100072.xml	timeseries/CHABA.txt	2033 \pm 4
CCE2	ocads/data/0084099.xml	timeseries/CCE2.txt	2028 \pm 3
Dabob	ocads/data/0116715.xml	NA	2050 \pm 6
NH-10	ocads/data/0157247.xml	timeseries/NH10.txt	NA ^a
Twanoh	ocads/data/0157600.xml	NA	2050 \pm 6
Ala Wai	ocads/data/0157360.xml	timeseries/ALAWAL.txt	2024 \pm 3
Chuuk	ocads/data/0157443.xml	timeseries/CHUUK.txt	2021 \pm 2



CRIMP1	ocads/data/0100069.xml	timeseries/CRIMP1.txt	2022 ± 4 ^a
CRIMP2	ocads/data/0157415.xml	timeseries/CRIMP2.txt	2030 ± 3
Kaneohe	ocads/data/0157297.xml	timeseries/KANEOHE.txt	NA
Kilo Nalu	ocads/data/0157251.xml	timeseries/KILONALU.txt	2017 ± 2
Gray's Reef	ocads/data/0109904.xml	timeseries/GRAYSREEF.txt	2027 ± 3
Gulf of Maine	ocads/data/0115402.xml	timeseries/GULFOFMAINE.txt	2023 ± 3
Crescent Reef	ocads/data/0117059.xml	timeseries/CRESCENTREEF.txt	2020 ± 2
Hog Reef	ocads/data/0117060.xml	timeseries/HOGREEF.txt	2023 ± 3
Coastal MS	ocads/data/0100068.xml	timeseries/COASTALMS.txt	2046 ± 7
Cheeca Rocks	ocads/data/0157417.xml	timeseries/CHEECAROCKS.txt	2020 ± 2
La Parguera	ocads/data/0117354.xml	timeseries/LAPARGUERA.txt	2019 ± 2

Notes: a Discontinued sites where a long-term trend cannot be quantified solely from this time series data product. b Links to NCEI archived deployment-level data files are provided for both MOSEAN and WHOTS; however, these time series are combined in the time series data product.



5 **Figure 1:** Location of (a) 40 moored $p\text{CO}_2$ time series with insets enlarged for the (b) U.S. West Coast and (c) Hawaiian Island of Oahu. Circle color represents climatological mean seawater $p\text{CO}_2$ (μatm), size of circle represents seasonal amplitude, and thickness of circle outline represents interannual variability (IAV). Gray squares show the locations of JKEO, M2, and NH-10 where insufficient winter observations prevent the calculation of climatological mean or seasonal amplitude. IAV is not shown for sites with less than 3 years of observations (Kaneohe, Iceland, BOBOA, SEAK, M2, SOFS, BTM, TAO165E, TAO155W, NH-10, and JKEO). Dabob and Twanoh data shown here are $x\text{CO}_2$ ($\mu\text{mol mol}^{-1}$).

10

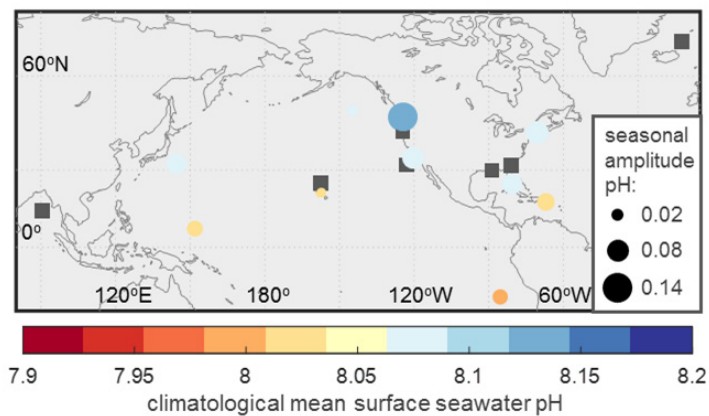


Figure 2: Location of 17 moored pH time series. Circle color represents climatological mean seawater pH and size of circle represents seasonal amplitude. Gray squares show the locations of moored pH time series where lack of seasonal distribution of measurements prevent the calculation of climatological mean or seasonal amplitude.

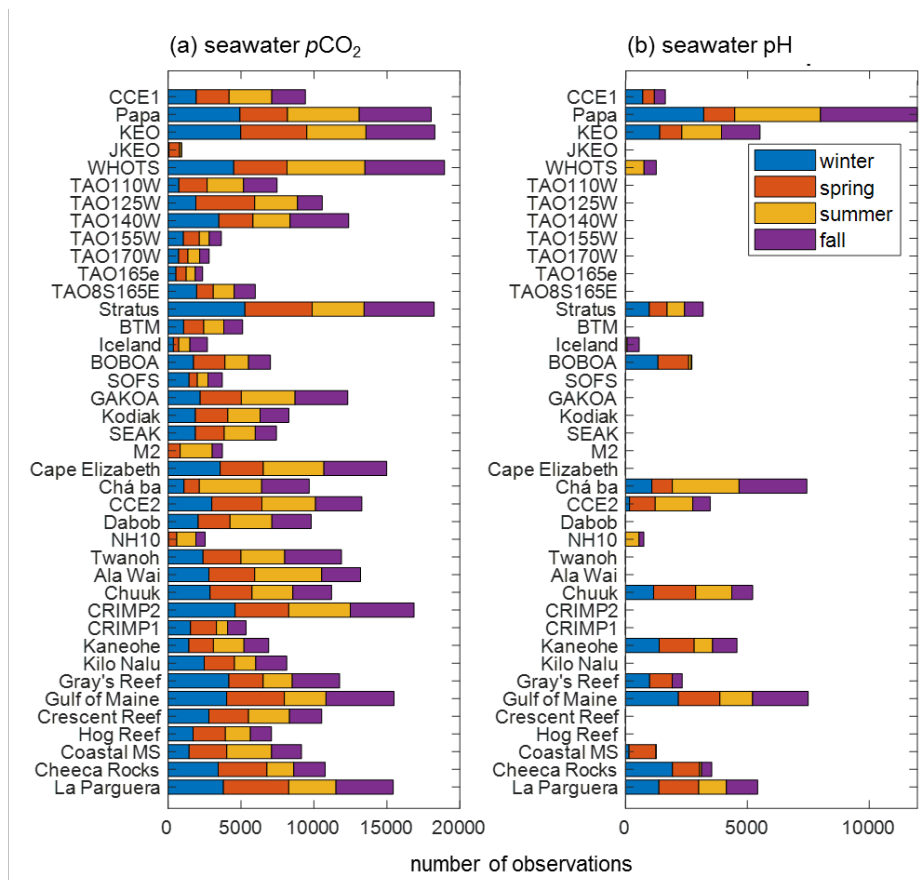


Figure 3: Number of surface seawater (a) $p\text{CO}_2$ and (b) pH observations by season in each of the 40 moored time series. For Northern Hemisphere sites, winter is defined as December, January, February; spring is March, April, May; summer is June, July, August; and fall is September, October, November (seasons reversed for Southern Hemisphere sites). Number of observations for Dabob and Twanoh shown here are seawater $x\text{CO}_2$.

5

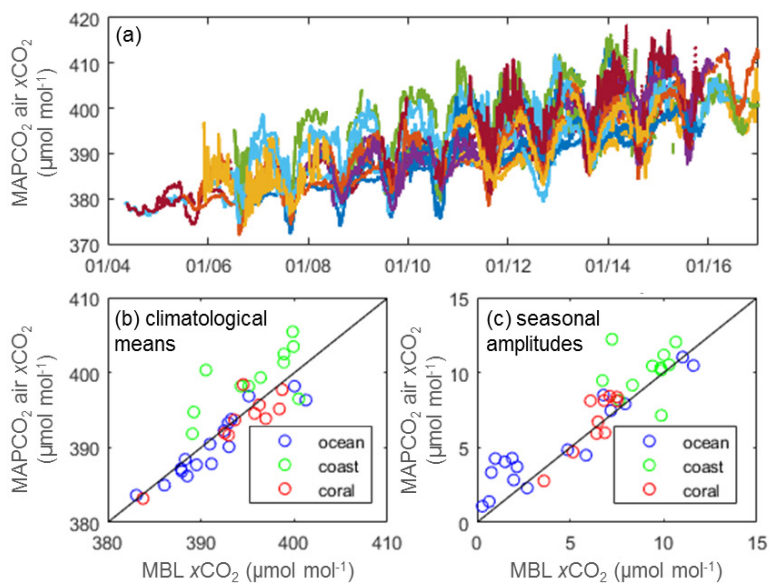


Figure 4: (a) Weekly averaged air $x\text{CO}_2$ observations from the 40 time series. Different colors represent each time series. Dates are MM/YY. (b) Climatological means and (c) seasonal amplitudes of air $x\text{CO}_2$ from the MAPCO₂ measurements compared to the GLOBALVIEW-CO2 MBL data product (GLOBALVIEW-CO2, 2013) for open ocean (blue), coastal (green), and coral reef (red) time series locations.

5

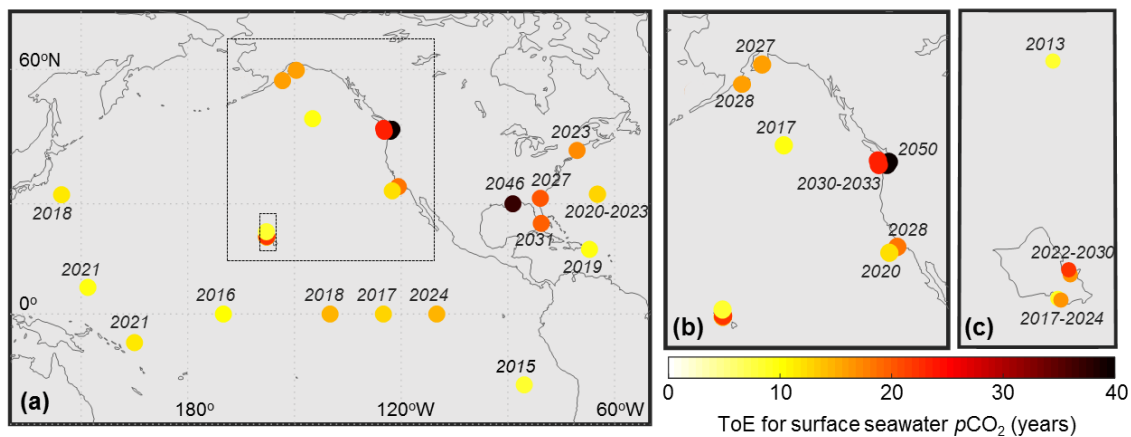


Figure 5: (a) Time of emergence (ToE) estimates in years with insets enlarged for the (b) U.S. West Coast and (c) Hawaiian Island of Oahu. ToE is not shown for sites with less than 3 years of observations (Kaneohe, Iceland, BOBOA, M2, SEAK, SOFS, BTM, TAO165E, TAO155W, NH-10, and JKEO). Years shown are the earliest dates of seawater $p\text{CO}_2$ trend emergence for each time series, which is the ToE estimate plus the time series start year (Table 1). These years of trend emergence and associated uncertainty are also shown in Table 2.

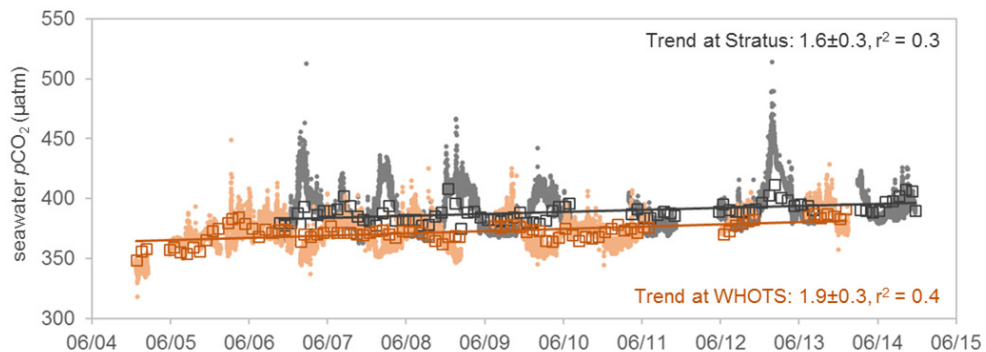


Figure 6: Surface seawater $p\text{CO}_2$ (μatm) 3-hourly observations (dots), deseasoned monthly anomalies (squares), and trend (lines) for the Stratus (gray) and WHOTS (orange) time series. Dates are MM/YY.